13911

COMPUTATIONAL MODELING OF AGE-DIFFERENCES IN A VISUALLY DEMANDING DRIVING TASK: VEHICLE DETECTION.[1]

R. Darin Ellis[2], Thomas Meitzler[3], Gary Witus[4],

Euijung Sohn[3], Darryl Byrk[3], Richard Goetz[3] and Grant Gerhart[3]

RUNNING HEAD: Modeling Vehicle Detection

Report Documentation Page

Form Approved
OMB No. 0704-0188

1. REPORT DATE	2. REPORT TYPE	3. DATES COVERED
07 OCT 1997	**Technical Report**	**07-10-1997 to 07-10-1997**

4. TITLE AND SUBTITLE
Computational Modeling of Age-Differences In a Visually Demanding Driving Task: Vehicle Detection

5a. CONTRACT NUMBER

5b. GRANT NUMBER

5c. PROGRAM ELEMENT NUMBER

6. AUTHOR(S)
Thomas Meitzler; Darryl Bryk; Richard Goetz; Grant Gerhart; Euijung Sohn

5d. PROJECT NUMBER

5e. TASK NUMBER

5f. WORK UNIT NUMBER

7. PERFORMING ORGANIZATION NAME(S) AND ADDRESS(ES)
U.S. Army TARDEC ,6501 E.11 Mile Rd,Warren,MI,48397-5000

8. PERFORMING ORGANIZATION REPORT NUMBER
#13911

9. SPONSORING/MONITORING AGENCY NAME(S) AND ADDRESS(ES)
U.S. Army TARDEC, 6501 E.11 Mile Rd, Warren, MI, 48397-5000

10. SPONSOR/MONITOR'S ACRONYM(S)

11. SPONSOR/MONITOR'S REPORT NUMBER(S)
#13911

12. DISTRIBUTION/AVAILABILITY STATEMENT
Approved for public release; distribution unlimited

13. SUPPLEMENTARY NOTES

14. ABSTRACT
While older adults experience fewer automobile accidents than the rest of the population their crash rate per mile driven parallels that of new drivers. Many accidents can be linked to visual detection problems, e.g., not seeing a car approaching at an intersection. The visual task of detecting an approaching vehicle was modeled with a neuro-physiologically motivated computational simulation of early vision, the National Automotive Center - Visual Perception Model (NAC-VPM). The scientific literature documenting age-related changes in early vision was reviewed in relationship to the components of the N AC-VPM, and the model was fit to lab data from older observers. The model fit the older observers' data adequately, particularly when the data was partitioned into subsets based on viewing conditions. Model fits were compared to calibrations based on younger observers' data. The calibrations based on older observers were substantially different from calibrations based on younger observers, indicating that the model can capture age-related differences in visual perception. When calibrated to the older adults' data, the model successfully predicted conditions under which vehicle detection was particularly difficult for older adults.

15. SUBJECT TERMS

16. SECURITY CLASSIFICATION OF:			17. LIMITATION OF ABSTRACT	18. NUMBER OF PAGES	19a. NAME OF RESPONSIBLE PERSON
a. REPORT	b. ABSTRACT	c. THIS PAGE			
unclassified	**unclassified**	**unclassified**	**Same as Report (SAR)**	**31**	

COMPUTATIONAL MODELING OF AGE-DIFFERENCES IN A VISUALLY DEMANDING DRIVING TASK: VEHICLE DETECTION.

ABSTRACT

While older adults experience fewer automobile accidents than the rest of the population, their crash rate per mile driven parallels that of new drivers. Many accidents can be linked to visual detection problems, e.g., not seeing a car approaching at an intersection. The visual task of detecting an approaching vehicle was modeled with a neuro-physiologically motivated computational simulation of early vision, the National Automotive Center – Visual Perception Model (NAC-VPM). The scientific literature documenting age-related changes in early vision was reviewed in relationship to the components of the NAC-VPM, and the model was fit to lab data from older observers. The model fit the older observers' data adequately, particularly when the data was partitioned into subsets based on viewing conditions. Model fits were compared to calibrations based on younger observers' data. The calibrations based on older observers were substantially different from calibrations based on younger observers, indicating that the model can capture age-related differences in visual perception. When calibrated to the older adults' data, the model successfully predicted conditions under which vehicle detection was particularly difficult for older adults.

COMPUTATIONAL MODELING OF AGE-DIFFERENCES IN A VISUALLY DEMANDING DRIVING TASK: VEHICLE DETECTION.

INTRODUCTION

Older Drivers

Approximately 13% of the driving population is over the age of 65. While the older segment of the driving population travels fewer miles and has fewer drivers involved in crashes, the risk per-mile-driven parallels that of teen drivers [20]. Even more troubling is that older drivers are more fragile than their younger counterparts. When measured in terms of fatalities per year per driver, older drivers are at approximately the same risk of death as the rest of the population. However, when measured per mile driven, the older population has a much greater risk of dying: Compared to 20 year-olds, drivers 75 and older are 3 times as likely to die in a given crash [20].

Most crashes occur at intersections, across all age groups. The proportion of crashes which occur at intersections, however, are highest for older drivers. Approximately 60% of older drivers' accidents are involved directly with an intersection [20]. Patterns of driver error are different across age groups as well. Older adults are less likely to be involved in an accident where excessive speed is to blame, however, they fail to yield right-of-way at twice the rate of younger drivers (18%, compared to 9%; [20]). Older drivers also have almost twice the rate of errors at signed or signalized intersections (14% vs. 9% of younger drivers; [20]). Self-reports indicate that older drivers consider these driving situations difficult, particularly among females and for drivers over the age of 75 [3].

The epidemiological statistics cited above have led researchers to ask the question, "Why do older drivers get in accidents?" Various hypotheses have been proposed to understand aspects of this phenomenon, including changes in risk perception [23] and declines in psychomotor ability (e.g., reaction time; [15]). In addition to these factors, the National Highway Traffic Safety Administration has made investigation of the role of vision in driving a research priority [20]. Researchers have estimated that the vast majority (as much as 90%), of the total input to a driver is visual [1, 8], and these demanding visual requirements have direct performance implications for older drivers. In a survey of 341 older adults, vision problems were reported to make driving difficult, particularly for drivers over the age of 75 [3]. Other researchers have noted the potential of visual perception as a predictor of older drivers' performance [17, 19, 21]. In a prospective study of crash involvement, Ball et al. [2], evaluated various measures of vision and visual information processing and found all of them superior to age as a predictor of accidents. The objective of this investigation was to use a computational model of early visual perception, the National Automotive Center—Visual Perception Model (NAC—VPM), to predict age-differences in a vehicle detection task. In the next section, the literature regarding age and vision is reviewed, drawing out the age-related changes which the NAC—VPM is equipped to accommodate.

Age-Related Changes in the Basic Properties of Vision

There are age-related changes in physiology andneurophysiology of the eye which impact all visual performance, including driving. Kline and Scialfa [10, 11] recently reviewed the literature, noting age-related changes in the cornea, aqueous humor, iris and pupil, lens, and vitreous humor. There is also evidence of photoreceptor cell loss, particularly in the parafoveal region [11]. Aging causes decreased retinal illumination and increased light scatter [22]. These two factors along with deficits in photo-pigmentation and the visual neural pathways, are responsible for a decreased light sensitivity among older adults, on the order of .09 log units per decade of life [10].

Contrast sensitivity reaches its maximum in early adulthood. Although the variability in contrast sensitivity loss increases with age, the overall trend is steady decline [4, 16, 22]. For 70 year-olds to perform as well as 20 year-olds, therefore, the task contrast must be 1.7 to 2.4 times greater [4]. Aspects of spatial vision, linked to basic contrast sensitivity, also decline with age [18]. The contrast sensitivity function (CSF) is a clinical measure of an observer's ability to detect sinusoidal gratings at different spatial frequencies, measured in cycles per degree of visual angle (c/deg). The contrast between the lightest and darkest portions of the grating specify the contrast, and the contrast required for detection varies with the grating's spatial frequency. Sekuler and Owsley [18] tested 100 observers across the adult life span. They found that for low spatial frequencies (.5-1.0 c/deg), all ages performed equally well. However, at higher spatial frequencies (starting at about 4 c/deg) the performance of older adults began to drop relative to their younger counterparts. Further, the spatial frequency which produced peak sensitivity dropped from 4 c/deg in 20 year-olds to 2 c/deg in 60 year-olds. Similar findings from other research are summarized in Kline and Scialfa [11].

Aging also brings declines in motion sensitivity. As with contrast sensitivity, the age differences in temporal resolution vary with spatial frequency characteristics of the target. For low spatial frequencies there is no evidence for age-effects, however, as spatial frequency increases, temporal resolution declines markedly [10]. However, many of the laboratory studies investigating the age-related decline in motion sensitivity do not address the extent to which older adults are disadvantaged under more ecologically valid circumstances. Some studies investigating the ability of older adults to judge the speed of an approaching vehicle have shown that older adults perform as well as younger adults [11].

Compared to other aspects of vision, color discrimination is fairly stable with age, although there is still some decline in sensitivity. In particular, older adults have exhibited errors on the blue/yellow axis of the Farsworth/Munsell 100 Hue Test, and the blue/green discrimination of the Lanthony New Color Test [10]. Evidence suggests that there are both optical components (e.g., changes in the light absorbing characteristics of the lens and cornea) and neural components (e.g., changes in photo-pigment density) in this decline.

Modeling the Role of Aging and Vision in Driving: Vehicle Detection

Recent advances have been made in computational modeling of object detectability in naturalistic scenes. The NAC-VPM was developed at the US Army Tank-automotive and Armaments Command (TACOM) to analyze detectability according to the mechanisms of visual perception. The NAC-VPM has been used extensively by the military to model data across a wide range of signature and visibility conditions. The NAC-VPM simulates the operation of the "early" stages of visual processing, from the retinal image to the neural receptive field (RF) response. The model uses the output of these stages as inputs to a statistical decision model calibrated to task performance.

The model computes a target metric and predicts the detectability, d', for an experimenter-designated region in a given image. The model also produces "images" of the neural receptive field response over the image, by (1) spatial frequency channel, (2) temporal channel, and (3) luminance/color opponent channel. The d' measure is a standard psychophysical measure of signal detectability, independent of the observer's response bias. The target metric is a measure of how much information is available for subsequent observer decision making and response selection across all three channels in the region of the target. The current model does not predict search behavior or performance.

Color processing. Prior to simulating human color vision, the model converts the digital RGB images into standard XYZ color coordinates. Color vision is modeled as a two-stage process: first the image is processed by cones with short, medium, and long (SML) spectral sensitivity [5], followed by luminance and color-opponent receptive fields. At the present time both of these transformations are represented by simple 3-by-3 linear coordinate transformations from XYZ to SML, then from SML to luminance/color-opponent channels, subsequently denoted by black-white [BW], red-green [RG] and yellow-blue [YB].

Temporal filtering. The model simulates the retinal temporal response using three temporal filters: one lowpass and two bandpass after Mandler and Makous [14]. The parameters of the temporal filtering module were fit to temporal contrast sensitivity data from Kelly reprinted in DeValois and DeValois [6]. Current theory proposes that the visual system processes the time stream of imagery on the retina by sampling and then temporally filtering the images with lowpass and bandpass filters [6]. Sampling is punctuated by saccadic eye movements, which occur at intervals from 0.125 to 0.5 seconds. Temporal filtering occurs via the differential rates of adaptation by the transient response neural receptive field cells. Subsequently, color processing employs both the temporal lowpass and bandpass components [6]. Mandler and Makous [14] modeled this processing with a lowpass filter and two bandpass filters: (1) the lowpass filter has a 50% response cutoff at 8 Hz; (2) the mid-frequency bandpass filter has lower and upper 50% response points at 2 Hz and 15 Hz, respectively, and is centered at their approximate geometric mean (5.5 Hz); (3) the high-frequency bandpass filter has lower and upper 50% response points at 5 Hz and 30 Hz and is centered at their approximate geometric mean (12 Hz).

Following Mandler and Makous, the NAC—VPM also uses a lowpass and two bandpass filters. The input values of the temporal filters were obtained by fitting the model's cumulative response to the aggregate contrast sensitivity data from Kelly [9]. The NAC-VPM samples images within a window containing the experimenter-selected point in time to perform the temporal filtering. Three images result from the filtering of one image sequence: a lowpass image and two bandpass images.

Spatial Filtering. The NAC—VPM implements spatial filtering with a multi-resolution bandpass filter. Multi-resolution bandpass filtering is described in Landy and Movshon [12]. The NAC-VPM uses a sequence of spatial filters at one octave spacing between central frequencies and one-octave half-power full-bandwidth. The spacing between the central frequencies of the filters is prescribed by 4:1 subsampling. The bandwidth of the filters is governed by the convolution kernel: the kernel for multi-resolution spatial filtering is a 3-by-3 approximation to a radially symmetric bi-variate Gaussian. It produces unoriented "circular annulus" bandpass filtering.

Non-linear Receptive Field (RF) Response. The nonlinear RF response of the NAC—VPM is similar to that described by Landy and Movshon [12]. The NAC-VPM formulation normalizes the spatial bandpass output to the local average luminance (i.e., it divides the contrast by the luminance to derive the contrast ratio). The local average luminance is computed by applying a lowpass spatial filter to the temporal lowpass luminance image, adding a constant bias representing the "dark current" in the visual system, then applying multi-resolution lowpass filtering. The same luminance normalization Gaussian pyramid is used for all of the temporal/color channels.

NAC-VPM uses curves fit to contrast threshold data reprinted in DeValois and DeValois [6]. Meaningful contrast threshold data are available only for spatial frequencies from 0.25 c/deg to 32 c/deg. Since there is no human contrast threshold data to compare to outside this range, the accuracy of the NAC-VPM contrast threshold functions below 0.25 c/deg or above 32 c/deg is difficult to confirm.

The NAC-VPM computes the energy envelope of the contrast ratio spatial modulation. In the multi-resolution representation, squaring the contrast ratio yields the energy envelope (the multi-resolution subsampling scheme takes samples only where the imaginary frequency component of the frequency-domain representation is equal to zero). The energy envelope at each location is then normalized to the sum of the internal noise energy plus the local average energy. The internal noise energy is the square of the product of a gain parameter and a contrast threshold for each spatial frequency, temporal, and luminance/color-opponent channel.

The normalized energy is computed for the entire scene on all spatial, temporal and luminance/color-opponent channels. This normalized energy is the predicted RF response. The luminance normalization pyramid and the energy normalization pyramids are also stored for use later to compute the target's contribution to RF response.

<u>Target Contribution to RF Response</u>. On each spatial frequency, temporal and luminance/color-opponent channel, the NAC-VPM model computes the modulation due to the target by subtracting the local contrast ratio bias due to the background from the local contrast ratio for the original image.

An algorithm was developed and implemented using non-stationary multi-resolution spatial filtering to extrapolate the surrounding RBG pixel values into the target region. This procedure creates an image such that the content of target region does not add modulation to the image. On each multi-resolution plane, the algorithm replaces the modulation of the target region with the modulation induced solely by the surrounding scene, without using any target region image information. The contrast modulation from the target region is minimized in the sense that the apparent contrast modulation in the image is the same as if the observer's visual receptive fields were surgically modified so that they received no input from the target region.

The "background extrapolation" image serves as a baseline for determining the image modulation in the image due to contrasts created by the target. The contrast modulation in the target region of the "background extrapolation" is that induced by the surrounding scene, and the surrounding scene is identical to that of the original image Therefore, the contrast modulation on each visual channel due to the target is simply the difference in the multi-resolution spatial filter pyramids of the original (i.e., target present) and "background extrapolation" (i.e., target absent) images.

Aggregate Target Metric and Predicted Detectability. The target metric is the sum of the target contribution to RF detectability over the temporal and luminance/color-opponent channels of the spatial integrals. The target metric is a measure of the total RF response over all channels due to the target. The target detectability is computed as a linear function of the logarithm of the target metric. The logarithmic transformation is a common information-theoretic transformation [13]. The slope and intercept of the linear function are the task performance calibration parameters, and are estimated by linear regression of measured d' against the logarithm of the computed target metric.

This calibration approach assumes that the performance of the each visual subsystems, relative to each of the other subsystems does not vary significantly across tasks or individuals. The calibration is made at the system-level of model performance, rather than at the subsystem level. An adequate fit of the model to data generated from older observers would indicate that even when the visual system declines, the relative performance of various aspects of processing does not change.

Experimental Overview

The experimental task used the following scenario: The observer's vehicle was stopped at a four way intersection. Cross-traffic at this intersection did not stop. The task was to look in each direction, determine if there was a car coming from either (or both) directions, and make the appropriate response. In addition to intersections with stop signs, this scenario is similar to any location where the driver must stop, look and proceed if the way is clear.

Recall that intersection scenarios are disproportionately dangerous for older adults in terms of crash statistics, and that older drivers report high levels of difficulty with intersections compared to other driving situations. Given that age-related declines in vision are suspected to play a role in this phenomenon, the NAC-VPM was used to examine the performance of older drivers in this scenario.

The experiment was designed to investigate the effect of various scene and vehicle characteristics on the detectability of approaching vehicles at intersections, specifically among older drivers. Both a statistical model of detection performance and a calibration of the NAC-VPM were computed. Data for older observers were compared with results from an identical experiment conducted earlier with drivers aged 25-45 [24].

METHODS

Stimuli and Apparatus

Experimental control and data acquisition was accomplished with a LabVIEW virtual instrument running on an IBM-compatible PC. Inputs to the experimental control virtual instrument (ECVI) included stimulus information from a multimedia control computer (a Macintosh Quadra 950), participant-initiated experimental pacing information, and participant response information. Outputs from the ECVI included experimenter-initiated pacing information to the participant and instructions to the multimedia control computer. Stimuli were short video sequences staged and recorded at actual intersections, and presented with high-resolution thin-film-transistor LCD projectors using RGB input from laserdisk players. The imagery was rear-projected onto screens to the left, front, and right of the experimental participants. The entire display subtended a total of subtending a total of 184 degrees (wide) by 30 degrees (tall) of visual angle at a viewing distance of 2 meters. The front half of an automobile, or "car buck" was used as the participants' observation station

Participant input and response took place through two routes. First, a magnetic head tracker (MHT) provided real-time angular measurement of point-of-regard. Other participant-initiated input to the control computer's virtual instrument came from a custom-wired response pad. The configuration for the response pad included buttons for "target present," "unsure," and "target absent."

The stimuli were recorded with a SVHS camcorder at intersections of surface roads in rural Michigan. The camera was placed at the head position of a nominal driver stopped at the intersection. In all conditions the 0-degree (forward) orientation of the camera was due north.

The camera was leveled and then aimed at 76 degrees from the forward axis in both directions. There were three locations used for recording stimuli, referred to here as A, B, and C. Location A was a clear, open grassy area. Location B had some buildings and farm-equipment in the background. For locations A and B, scenes were recorded under clear morning (9:00 AM to 12:00 PM DST), clear afternoon (2:00 to 5:00 DST), and under overcast conditions in each direction. The combination of the sun's position in the sky and the direction being recorded allowed the AM and PM conditions to be recoded as "frontlit" (AM-left, PM-right) and "backlit" (AM-right, PM-left). Location C was a wooded area. For location C, the thick tree canopy created a "dappled" lighting effect on the road surface, and the images were all recorded within 120 minutes of solar noon under mostly sunny conditions. This combination produced fourteen combinations of background scene characteristics. There was no extraneous traffic in any of the recorded scenes. Under each combination of background characteristics, both target-absent and target-present scenes were recorded. For the target-present scenes three different vehicles were used: (1) a large black car; (2) a large white car; and (3) a small white car. Each of these cars made approaches to the intersection from each direction under four combinations of two factors: (1) with head lamps on and off; and (2) near and far.

Fourteen left-screen and right-screen images were randomly paired without replacement within each sky condition (representing each of the target characteristic cells and two corresponding no-target images), with the additional constraint that left- and right-screen images came from the same location. A total of four blocks of 56 images each were replicated in this manner. Each of these 4 blocks were then presented from left-to-right under the three different lab viewing conditions – unattenuated, neutral density filtered (reduced luminance), and filtered with back lighting (attenuated luminance and contrast). The random pairings were maintained, while presentation order was reversed for right-to-left displays. The four blocks of images were transferred from tape to laser compact disk for presentation through the laserdisk players.

Participants observed the stimulus imagery from the car buck. Adaptive and unobtrusive control of experimental pace was accomplished with the MHT: the participants turned their heads from side to side in a natural manner, activating a "switch" in the ECVI. The participants' response pad was integrated into the car buck's steering wheel. There were six response buttons in the response pad configuration. For both the left and the right side of a given experimental trial, the participants were able to respond, "Yes" (target present), "Not Sure," and "No" (no target present).

Participants

A total of 11 individuals were recruited from the general population, and were paid $150 for their participation. Participants were given a Snellen eye chart acuity screening and an Ishihara Color test to screen for any vision deficiencies. Participants were between the ages of 45 and 69, had a current driver's license, were high school graduates, and reported themselves as "in good health." Further, potential participants were screened out if they were commercial drivers, had three or more points on their license in the last five years, or if they were taking medication. Data for the comparison group of younger drivers, aged 25-35, was taken from an identical earlier experiment. There were 32 younger drivers, each of whom passed the same screening procedure.

Procedure

Following the screening test the subjects were shown a four-minute training tape which detailed the experimental protocol. Following the tape, each subject was provided with a 10-minute training session in the car buck. The experiment's average length was about three hours.

To avoid fatigue, each participant was provided with a break every 40 minutes and upon request during the experiment. After the presentation of a stimulus image, blue background was presented to reduce the possibility of eye strain during the test.

The presentation of the stimuli was arranged into four replicate imagery blocks. The presentation blocks corresponded to the three lab-manipulated lighting conditions. Each block of trials repeated the same sequence of intersection images. The duration of the video on the right and left screens in each trial was 240 ms (8 frames of video). A beep generated by the ECVI notified the participant to initiate a new trial. Trials were initiated via the MHT when the participant's head turned toward one of the projection screens. After participants looked in each direction and decided whether or not there was an approaching vehicle, they responded for each side with the response buttons on the steering wheel. Participants were instructed to be sure of their answers before responding, emphasizing accuracy over speed. Accuracy and its derivatives were the dependent measures used in all analyses.

Treatment of Data

The participant's responses were aggregated into a truth table by pairing the responses from each unique target present scene with the responses from corresponding target-absent backgrounds. These truth tables were used to calculate hit (P_{hit}) and false alarm (P_{fa}) rates for the observer population. By collapsing the uncertain responses into the "target present" responses for one analysis, and collapsing uncertain responses into target absent responses for a second analysis, we were able to calculate hit and false alarm rates at two response criterion levels (sure and unsure). The hit and false alarm rates were used to calculate two values of d' for each scene (one for each response criterion level). The overall estimate of d' for each scene was calculated from the two levels using the method described in MacMillan and Creelman [13].

RESULTS

Statistical Main Effects Among Older Observers

Initial analysis focused solely on the older drivers' data. Main effects were analyzed for the experimental factors among the older driver participant group using the General Linear Model (GLM) with SYSTAT 7.0. The older adults' detection sensitivities were significantly effected by Location [$F(2, 886) = 6.235$, $p = .002$], Scene lighting [$F(2, 886) = 54.198$, $p < .001$], Car color [$F(1, 886) = 14.403$, $p < .001$], Distance [$F(1, 886) = 130.889$, $p < .001$], and Luminance/ Contrast attenuation [$F(2, 886) = 145.032$, $p < .001$]. Overall the linear model of the main effects of these factors on older drivers' detection sensitivity (d') fit well, with a multiple $R = 0.728$. The average d' for older observers was 2.59, indicating good overall detection performance. The observers performed best at location B (mean d' = 3.01), not quite as well at location A (mean d' = 2.7), and worst at location C (mean d' = 1.31).

Across the various levels of scene lighting, d' varied even more widely. Overcast viewing conditions created the most favorable conditions for detection (mean d' = 3.29), followed by back-lighting (mean d' = 2.66) and front-lighting (mean d' = 2.45). The dappled viewing conditions of location C brought the lowest performance (mean d' = 1.31). Lab manipulation of contrast and luminance was the final background characteristic analyzed: performance was best when the image was left unmanipulated (mean d' =3.14) and worst when luminance and contrast were attenuated (mean d' = 1.87).

In addition to the effects of the various overall scene characteristics, target characteristics also played a role in performance. White vehicles were more detectable than black vehicles (mean d' = 2.69 vs. mean d' = 2.38, respectively). While car size did not have a significant main effect with the GLM, any positive effect of size may have been attenuated by averaging the d' values for the large black car with the large white car. Comparing means, the large white car was more detectable (mean d' = 2.99) than the smaller white car (mean d' = 2.20). Using a two-sample unequal variance t-test, the effect of car size was significant [$t(472) = 7.192$, $p < .001$]. For distance, vehicles which were farther away from the observer were more difficult to detect (mean d' = 2.1) compared to closer targets (mean d' = 3.08).

Statistical Effects of Age Group and Age Interactions

After analyzing the main effects of the experimental factors within the older observer group, the data were combined with that of 32 younger observers (aged 25-45). Once again, GLM was used to model the main effects for the combined data set. Additionally, the two-way interactions of experimental factors with Age group was modeled.

Although main effect for Age group failed to meet significance, Location [$F(1, 1772) = 15.5$, $p < .001$], Scene lighting [$F(3, 1772) = 116.1$, $p < .001$], Car color [$F(1, 1772) = 26.424$, $p < .001$], Distance [$F(1, 1772) = 325.520$, $p < .001$], and Luminance/contrast attenuation [$F(2, 1772) = 499.7$, $p < .001$] were significant. In accordance with the partitioned older age group analysis, Car size and Headlamps were not significant in the overall GLM.

The pattern of Location's effect was identical to that seen in the partitioned analysis of the older participants: detection performance was best at location B (mean d' = 2.84), declined some at location A (mean d' = 2.62), and was worst at location C (mean d' = 1.65). Overcast scene lighting produced the highest d' values (mean d' = 2.98), followed by backlighting (2.72), and front lighting (mean d' = 2.4). Once again, dappled lighting produced substantially worse performance (mean d' = 1.65). The lab-based attenuation of contrast and luminance also followed the same pattern as above. The highest levels of performance occurred under unattenuated lighting (mean d' = 3.22) and the lowest levels of performance occurred with attenuated contrast and luminance (mean d' = 1.67). With regard to target characteristics, white cars were more visible than black (mean d' = 2.64 vs. mean d' = 2.35) and closer vehicles were more visible than more distant vehicles (mean d' = 3.03 vs. mean d' = 2.05).

While there was no overall difference between age groups, the Scene lighting X Age interaction [$F(3, 1772) = 31.3$, $p < .001$] and the Luminance/Contrast attenuation X Age interaction [$F(2, 1772) = 15.7$, $p < .001$] were significant. The observed d' values for both younger and older drivers during back-lit conditions were approximately the same. Again for the front-lit conditions, the younger drivers and the older drivers performed similarly. The differences were found under the overcast lighting and dappled conditions. The older drivers (mean d' = 3.29) were able to detect vehicles better than the younger drivers (mean d' = 2.67) during the overcast weather, whereas older drivers were less likely to detect a vehicle correctly under dappled lighting (mean d' = 1.31 vs. mean d' = 1.99).

The Luminance/contrast attenuation X Age interaction emerged in the following manner: Natural scene lighting (full luminance and contrast) resulted in lower observed d' values for older drivers(mean d' = 3.15) than for the younger drivers (mean d' = 3.3). Both age groups had lower detection sensitivity when the luminance and contrast were both attenuated in the lab. The older drivers' observed d' (mean d' = 1.87) was higher than the young adults' observed d' (mean d' = 1.47) under these manipulated conditions.

<u>Model Calibration</u>

As described above, the NAC-VPM computes a target metric from an image and associated photometric and neurophysiological data. The detectability metric, $d'_{predicted}$, is predicted from the target metric and two psychophysical parameters, **a** and **b**, using the following formula:

$$d'_{predicted} = \mathbf{a} * \ln(\text{TargetMetric}) + \mathbf{b} \qquad \textbf{(Eq. 1)}$$

The fit of the model to the observed data is measured by the correlation between the observed d' and the logarithm of the target metric. Since there are two estimates of d' for each case, one at the "Y" and one at the "Y or ?" response levels, a good estimate of d' is the sample mean [13]:

$$d'_{measured} = [d'(Y) + d'(Y + ?)]/2 \qquad \textbf{(Eq. 2)}$$

NAC-VPM is calibrated by fitting a linear regression of the logarithm of the target metric against observed d' to estimate the slope and intercept, **a** and **b.** The overall quality of the calibration is measured by the fit of the regression. The validity of the calibration is also tested by examining the shape of the probability distribution of the error between the predicted and measured d': ideally the distribution of residuals should be unimodal and Gaussian in shape.

The calibration data set consisted of 878 cases. There were 899 cases with subject response data, but the model could not be run for 21 cases because the image data files or associated target regions were corrupted.

For the 45 and older age group, the correlation of the logarithm of the target metric with the observed d' was $R = .48$ over the entire data set. The calibration regression was highly significant [$F(1, 876) = 264.22$, $p < .001$], while parameter values were **a** = 0.892 and **b** = -3.216. Compared to the younger observers, this fit was fairly low. The calibration regression for the younger age group was also significant [$F(1, 876) = 982.4$, $p < .001$], but indicated a relatively high correlation ($R = .73$) between observed and predicted d' values. The parameter values for the younger observers were **a** = 1.228 and **b** = -5.484.

Figure 1 is a histogram of the residuals for the older age group across the range of estimated values. A Kolmogorov-Smirnov test was used to analyze the standardized residuals. The observed distribution of standardized residuals did not differ from a Gaussian [0, 1] distribution ($p = .411$).

-- Figure 1 here --

While the residuals indicated that the model estimates were not systematically biased, the lower value of R, relative to the younger observers' calibration, indicated that the model was not adequately accounting for performance. We then examined the validity of the calibration across the various experimental factors. The calibration for all but one of the factors, Location, was comparable to that of the entire data set.

As noted previously, location C was selected for its unusual lighting conditions: the road at location C was covered by a tree canopy. There was some light coming through the tree canopy (i. e., the dappled lighting effect) which created an artificial "camouflage" pattern by superimposing a pattern on the car that was not characteristic of the car and was similar to the pattern on the ground. As Figure 2 shows, the model greatly over-estimated the detection ability of older observers under dappled lighting. Since this lighting effect was qualitatively different than that seen at the other two locations, the older observers' data was partitioned into two groups (location C vs. locations A & B).

-- Figure 2 here --

Location C – Calibration. There were 143 cases at location C. For the 45 and older age group, the correlation between predicted and observed d' was much better, with $R = .764$. The calibration regression was highly significant [$F(1, 876) = 197.91$, $p < .001$] with parameter values of $\mathbf{a} = 1.211$ and $\mathbf{b} = -6.855$. By comparison, the calibration regression for the younger age group was also significant [$F(1, 141) = 290.45$, $p < .001$], and indicated a relatively high correlation ($R = .82$) between observed and predicted d' values. The parameter values for the younger observers were **a** = 1.382 and **b** = -7.323.

Locations A & B – Calibration. There were 733 cases at the location A & B sites. For the older observers, the correlation between model predictions and observed performance was 0.57. The calibration regression was significant [$F(1, 733) = 351.43$, $p < .001$], with parameter estimates of **a** = 0.989 and **b** = -3.554. The calibration of the model with younger observers' data, on the other hand, maintained a correlation comparable with that of the entire data set [$F(1, 733) = 1025.37$, $p < .001$, $R = .764$, **a** = 1.285 and **b** = -5.692]. The fit of the model to the older observers' data once again improved, but not to the extent seen with the calibration of location C.

DISCUSSION

The statistical and computational modeling analyses of vehicle detection at an intersection complement each other to provide a deeper understanding of performance than that which could be provided by either on its own. The statistical modeling demonstrated which environmental and vehicle characteristics have an effect on real-world target detection performance. Further, we have found that under some circumstances, older drivers are not at a deficit in terms of performance, while under other circumstances (e.g., dappled lighting) detection performance suffers disproportionately. Most important is that the modeling approach used in concert with knowledge of basic changes in vision with age contributes an understanding of the mechanisms of declining task performance, i. e., the model tells us that older adults perform poorer than younger adults in this vehicle detection task due to differences in spatial, temporal, and color/luminance sensitivity. It is important to note here that the model fit the data best in the situation which produced the worst task performance in older adults.

There were no main effects for age in the present experiment. Most other research investigating the role of age and vision in driving tasks has found an age main effect. There are two main reasons why this might have been the case. First, the older group was limited to 11 participants, thus the lack of a main effect could have been due to a lack of statistical power and less stable estimates of hit and false alarm rates (relative to the younger observers). Secondly, the present experiment was limited by a wide age range (from age 45 to 69) in the present data. This could also have contributed to relatively unstable estimates of hit and false alarm rates. However, a lack of age differences is not without precedence; Guerrier et al. [7] found that age was not a good predictor of performance in a driving simulator.

While the difficulty of location C was predicted due to the artificial camouflage effect, the relative difficulty of locations A and B were unexpected. The farm equipment in the background of location B was expected to cause higher false alarm rates, and corresponding lower d' values, compared to the grassy open area of location A. However, the grassy location proved to be more difficult. In retrospect, the farm equipment was fairly easy to ignore, and the grass on the shoulder of the road at location A was distracting, perhaps due to wind movement. The remainder of the significant statistical main effects were in the expected direction.

Across the other experimental factors, vehicles which had their headlamps on were no more visible than those with headlamps off in the current experiment. The model predictions, however, concurred with statistical performance estimates: headlamps contributed only a very marginal proportion to the overall target metric. One speculative explanation is that the imagery, as projected in the lab, was not an accurate rendering of the illuminance of headlamps under on-the-road conditions. The model was calibrated with photometric data taken from the rear-projection screens, rather than from environmental spectro-photometric readings. Future work is required to investigate the effect of headlamps under more realistic viewing conditions.

Overall the NAC-VPM provided better predictions of performance for the younger participants. As mentioned above, the older group had much larger performance variability than the younger group. Given these circumstances, the fact that the model fit the data is a testament to the model's robustness. However, it is important to note that while the model fit the younger data better, the increase in fit achieved by partitioning the data was much more dramatic for the older observers: the fit improved considerably for the dappled lighting conditions of location C. This is important because location C was the most difficult scenario for both groups, disproportionately so for older observers. Thus the model performed best in the area where it can do the most good, in terms of contributing to an understanding of the problem and providing guidance for the design of effective countermeasures.

While the partitioned analyses demonstrated that one calibration will not work for every condition, it is also evident that one global calibration (which works well for younger drivers) will not necessarily work well for all age groups. The parameter differences between age groups were notable, thus, trying to predict performance in a population of older drivers with a model calibrated for younger drivers is clearly an inadequate approach.

CONCLUSION

Overall, the NAC-VPM shows promise as a tool to investigate age-differences in driving-related visual performance. As the older driving population continues to grow, it will become even more important to understand the barriers to their continued mobility and independence.

Future work with the NAC-VPM will account for potential variation in decline across the various modules of the model: color processing, and spatial and temporal filtering. Future research should focus on the role of design countermeasures such as variable intensity brake lights, glass treatments, and daytime running lights. With an understanding of age-differences in performance, designers can find interventions which will help keep older drivers safely on the road.

FOOTNOTES

[1] Manuscript received ____________________. This work was supported in part by the National Automotive Center, US Army TACOM, Warren, MI.

[2] Corresponding Author: Dr. R. Darin Ellis, Institute of Gerontology and Department of Industrial and Manufacturing Engineering, 87 E Ferry St. 226 Knapp Building, Wayne State University, Detroit, MI, 48202. Email: ellis@iog.wayne.edu

[3] US Army, Tank-automotive and Armaments Command, Warren, MI

[4] Turing Associates, Ann Arbor, MI

REFERENCES

[1] I. L. Bailey, & J. E. Sheedy, "Vision screening for driver licensure," Transportation in an Aging Society, vol 2., special report #218, Washington DC: Transportation Research Board, 1988.

[2] K. Ball, C. Owsley, D. Roenker, & M. Sloane, "Isolating risk factors for crash frequency among older drivers," Proceedings of the Human Factors Society 37th Annual Meeting, pp. 211-214, Santa Monica CA: HFES, 1993.

[3] R. R. Bishu, B. Foster, & P. T. McCoy, "Driving habits of the elderly - a survey," Proceedings of the Human Factors Society 35th Annual Meeting, pp. 1134-1138, Santa Monica CA: HFES, 1991.

[4] O. M. Blackwell & H. R. Blackwell, "Visual performance data for 156 normal observers of various ages," Journal of the Illumination Engineering Society, vol. 1, pp. 3-13, 1971.

[5] R. M. Boynton, Human Color Vision, 1992, New York:Optical Society of Americaa

[6] R. L. DeValois & K. K. DeValois, Spatial Vision, 1990, Oxford: Oxford University Press.

[7] J. Guerrier, P. Manivannan, A. Pacheco, F. L. Wilkie, "The relationship of age and cognitive characteristics of drivers to performance of driving tasks on an interactive driving simulator," Proceedings of the Human Factors and Ergonomics Society 39th Annual Meeting, 1995.

[8] B. L. Hills, "Vision, visibility, and perception in driving," Perception, vol. 9, pp. 183-216, 1980.

[9] D. H. Kelly, "Visual responses to time dependent stimuli: I. Amplitude and sensitivity measurements," Journal of the Optical Society of America, vol. 51, pp. 522-529, 1961.

[10] D. W. Kline, & C. T. Scialfa, "Visual and auditory aging," In J. Birren & K. W. Schaie (Eds.) Handbook of the Psychology of Aging (4th edition), 1996, New York: Academic Press.

[11] D. W. Kline, & C. T. Scialfa, "Sensory and perceptual functioning: Basic research and human factors implications," In A. D. Fisk, W. A. Rogers, and N. Walker (Eds.) Handbook of Human Factors and the Older Adult, 1997, New York: Academic Press.

[12] M. S. Landy & A. J. Movshon, Computational models of Visual Processing, 1991, Boston MA: MIT Press.

[13] N. A. MacMillan & C. D. Creelman, Detection Theory: A User's Guide, 1991, Cambridge: Cambridge University Press.

[14] M. B. Mandler & W. Makous, "A three channel model of temporal frequency perception," Vision Research, vol. 24, pp. 1881-1887, 1984.

[15] T. Mast, "Designing and operating safer highways for older drivers: Present and future research issues, Proceedings of the Human Factors Society 35th Annual Meeting, pp. 1139-1143, Santa Monica CA: HFES, 1991.

[16] D. G. Pitts, "The effects of aging on selected visual functions: Dark adaptation, visual acuity, stereopsis, and brightness contrast," In R. Sekuler, D. Kline, and K. Dismukes (Eds.), Aging and Human Visual Function, 1982, New York: Alan R. Liss.

[17] F. Schieber, D. W. Kline, T. J. B. Kline, & J. L. Fozard, "The relationship between contrast sensitivity and the visual problems of older drivers," SAE Technical Paper Series, SAE 92-0163, Warrendale PA: SAE, 1992.

[18] R. Sekuler & C. Owsley, "The spatial vision of older humans," In R. Sekuler, D. Kline, & K. Dismukes (Eds.), Aging and Human Visual Function, 1982, New York: Alan R. Liss.

[19] J. P. Szlyk, "Relative effects of age and compromised vision on driving performance," Human Factors, vol. 37, no. 2, pp. 430-436, 1995.

[20] US Department of Transportation (1993). Addressing the Safety Issues Related to Younger and Older Drivers. Report to Congress January 19, 1993. Washington DC: US DOT -- National Highway Traffic Safety Administration.

[21] J. Walker, C. Sedney, K. Wochinger, D. A. Boehm-Davis, & W. A. Perez, "Age differences in the useful field of view in a part-task driving simulator," Proceedings of the Human Factors Society 37th Annual Meeting, pp. 960-963, Santa Monica CA: HFES, 1993.

[22] R. A. Weale, "Retinal illumination and age," Transactions of the Illumination Engineering Society, vol. 26, pp. 95-100, 1961.

[23] D. J. Winter, "Older drivers – their perception of risk," SAE Technical Paper Series, SAE 88-1752, Warrendale PA: SAE. 1988.

[24] G. Witus, "TARDEC National Automotive Center Visual Perception Model (NAC-VPM)," Final Report under contract DAAE07-94-C-R111 to US Army Tank Automotive and Armaments Command, December 26, 1996.

Figure Captions

Figure 1. Histogram of residuals for older observers over entire data set. Kolmogorov-Smirnov test showed that the distribution of residuals was not significantly different from Gaussian [0,1], $p=.411$

Figure 2. Model fits across locations for older observers.

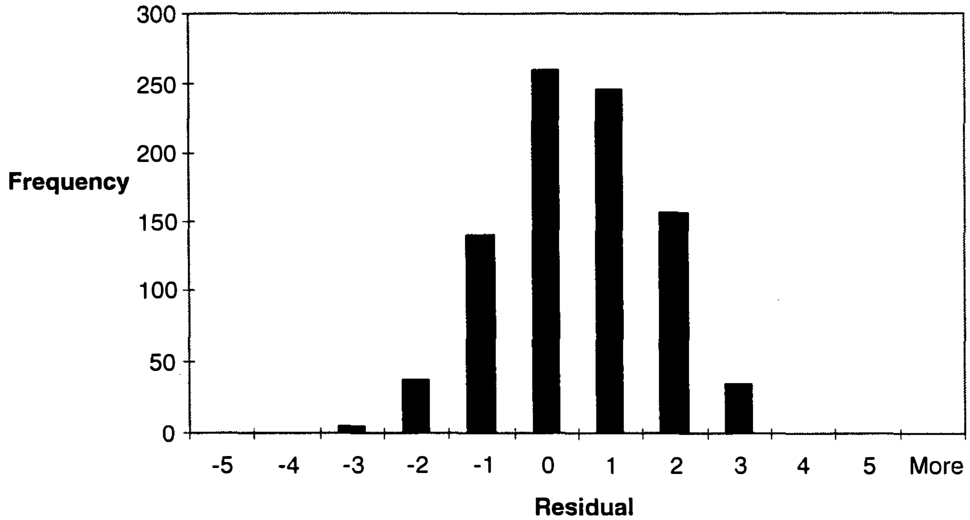
300
250
200
Frequency
150
100
50
0
-5
-4
-3
-2
-1
0
1
2
3
4
5
More
Residual

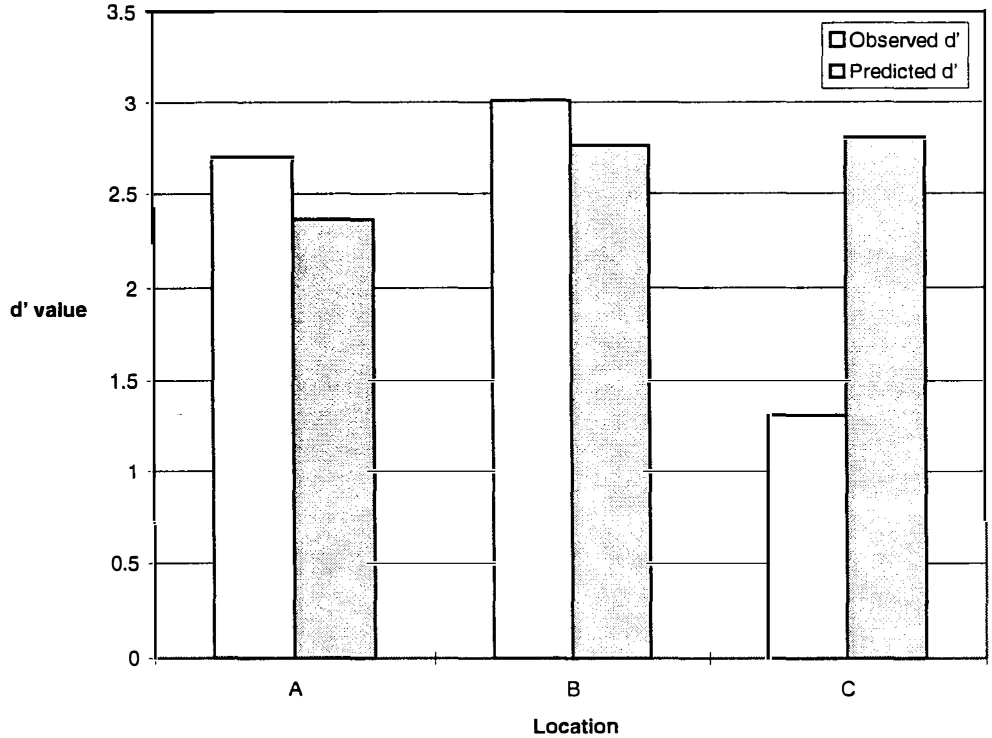
Observed d'
Predicted d'
3.5
3
2.5
2
1.5
1
0.5
0
d' value
A
B
C
Location